2004

The large-scale bias of the hard X-ray background

Stephen P. Boughn
Haverford College, sboughn@haverford.edu

R. G. Crittenden

The Astrophysical Journal, 612:647–651, 2004 September 10

THE LARGE-SCALE BIAS OF THE HARD X-RAY BACKGROUND

S. P. Boughn
Department of Physics, Princeton University, Princeton, NJ 08544; and Department of Astronomy, Haverford College, Haverford, PA 19041; sboughn@haverford.edu

and

R. G. Crittenden
Institute of Cosmology and Gravitation, University of Portsmouth, Portsmouth PO1 2EG, UK; robert.crittenden@port.ac.uk
Received 2004 March 17; accepted 2004 May 19

ABSTRACT

Recent deep X-ray surveys combined with spectroscopic identification of the sources have allowed the determination of the rest-frame 2–8 keV luminosity as a function of redshift. In addition, an analysis of the *HEAO 1* A-2 2–10 keV full-sky map of the X-ray background reveals clustering on the scale of several degrees. Combining these two results in the context of the currently favored ΛCDM cosmological model implies an average X-ray bias factor b_X of $b_X^2 = 1.12 \pm 0.33$, i.e., $b_X = 1.06 \pm 0.16$. These error estimates include only statistical error; the systematic error sources, while comparable, appear to be subdominant. This result is in contrast to the large biases of some previous estimates and is more in line with current estimates of the optical bias of L_* galaxies.

Subject headings: large-scale structure of universe — X-rays: galaxies — X-rays: general

1. INTRODUCTION

An important test of any cosmological model is that it be consistent with the observed distribution of matter in the universe. Since our primary knowledge of this distribution comes from observations of galaxies, it is essential to understand the extent to which galaxies trace the matter density. This relationship is usually quantified by a bias factor that relates fluctuations in the galaxies to those in the dark matter. It is complicated by the fact that the relation between the luminosity of a galaxy or groups of galaxies and the underlying distribution of matter can depend on the type of galaxy, the spectral band of the observation, the redshift z, and the scale length on which the comparison is made. However, such complications are also opportunities in that models of galaxy formation must successfully reproduce these differences.

The standard definition of the bias factor b is the ratio of the fractional galaxy density fluctuations to the fractional matter density fluctuations, i.e.,

$$b = \frac{\delta\rho_g/\rho_g}{\delta\rho/\rho}, \tag{1}$$

where ρ_g is the mean density of galaxies, ρ is the mean density of matter, and δ indicates the rms fluctuations of the densities about these means. If galaxies formed early ($z > 1$), as appears to be the case (e.g., Ellis 1997), then there are good reasons to expect that for linear density perturbations (i.e., $\delta\rho/\rho \ll 1$) on large scales in the nearby ($z \lesssim 1$) universe, galaxies should be relatively unbiased ($b \to 1$) tracers of the density field (Fry 1996; Tegmark & Peebles 1998); however, this assertion must be tested.

Here we focus on determining the bias of the hard X-ray background (XRB), which is known to be dominated by distant ($z \lesssim 2$) active galaxies and so provides a probe of the bias on large scales. The observed clustering of the XRB, when combined with what is known about the level of perturbations and the cosmological model from cosmic microwave background (CMB) observations, allows us to place relatively strong constraints on the X-ray bias.

Previous determinations of X-ray bias have resulted in a wide range of values, $1 < b_X < 7$ (see Barcons et al. 2000 and references therein). Some spread in the estimates is to be expected; e.g., at lower energies X-ray emission is dominated by clusters of galaxies and so are expected to be as highly biased as clusters themselves (Bahcall & Soneira 1983). However, another major contribution to the uncertainty in the bias estimates is the lack of accurate determinations of the clustering of various X-ray sources. Two of the lower estimates of X-ray bias are from Treyer et al. (1998), who found that $b_X \sim 1$–2 from a low-order multipole analysis of the *HEAO 1* A-2 data set, and Carrera et al. (1998), who found that the ratio of the X-ray bias of active galactic nuclei (AGNs) to that of *IRAS* galaxies to be $0.8 \lesssim b_X/b_I \lesssim 1.7$ from *ROSAT* observations. The remaining uncertainty in these determinations arose from uncertainties in both the X-ray luminosity function (LF) and in the cosmological model. Knowledge of both of these has improved dramatically in the last year, and this is largely responsible for the improved accuracy of the estimate of b_X in this paper.

2. CLUSTERING IN THE *HEAO 1* A-2 2–10 keV X-RAY MAP

We recently presented evidence of large-scale clustering in the *HEAO 1* A-2 2–10 keV full-sky map (Boldt 1987) of the hard XRB on angular scales of $\lesssim 10^\circ$ (Boughn et al. 2002). Before computing the correlations, local sources of the X-ray background were removed from the map. The map was masked to eliminate strong, nearby X-ray sources with fluxes exceeding 3×10^{-11} ergs s^{-1} cm^{-2}. In addition, all regions within 20° of the Galactic plane or within 30° of the Galactic center were masked. The map was also corrected for a linear time drift of the detectors, high Galactic latitude diffuse emission, emission from the local supercluster (Boughn 1999), and the Compton-Getting dipole. The latter components were fitted to and then

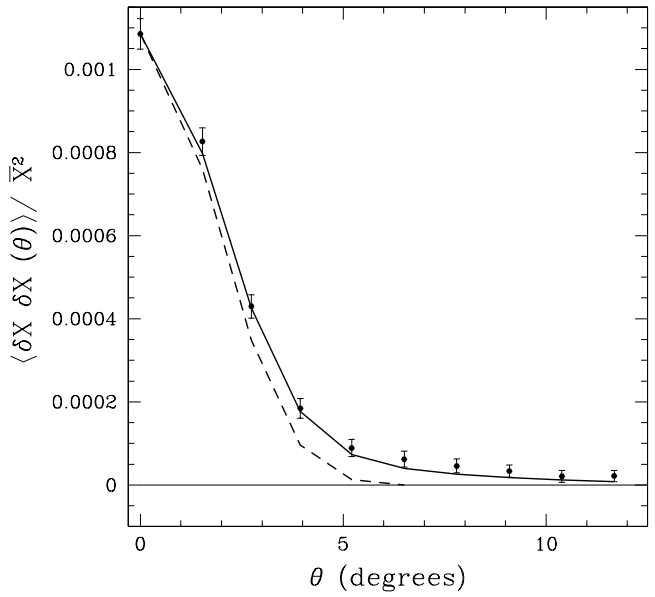

FIG. 1.—Autocorrelation function of the *HEAO 1* A-2 map with bright sources and the Galactic plane removed. The dashed curve is the form expected from beam smearing due to the PSF of the map, while the solid curve includes a contribution due to clustering in the XRB.

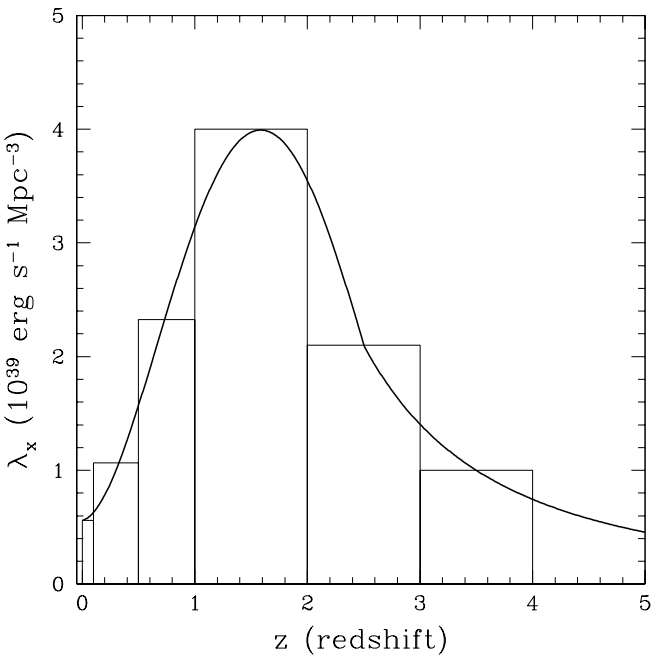

FIG. 2.—Volume emissivity as a function of redshift. The local value ($z = 0$) is the measurement of Miyaji et al. (1994). The low-redshift points are derived from the data of Steffen et al. (2003), while the high-redshift points ($z > 1$) come from Cowie et al. (2003).

removed from the map. Without these cuts and corrections, the correlations are dominated by a few strong point sources and large-scale diffuse structures in the map.

Figure 1 is a plot of the intensity angular correlation function (ACF) given by

$$\mathrm{ACF}(\theta) = \frac{1}{\bar{I}^2 N_\theta} \sum_{i,j} (I_i - \bar{I})(I_j - \bar{I}), \qquad (2)$$

where the sum is over all pairs of map pixels i, j separated by an angle θ, I_i is the intensity of the ith pixel, $\bar{I}$ is the mean intensity, and N_θ is the number of pairs of pixels separated by θ. Photon shot noise only appears in the $\theta = 0^\circ$ bin and has been removed. The highly correlated error bars were determined from 1000 Monte Carlo trials in which the pixel intensity distribution was assumed to be Gaussian with the same ACF as in the figure. The dashed curve represents the expected functional form of the contribution to the ACF due to telescope beam smearing of a random distribution of uncorrelated sources normalized to the ACF(0) point. It represents the profile that is expected if there were no intrinsic correlations in the XRB. The point-spread function (PSF) of the map is due to pixelization and to the finite telescope beam and was accurately determined from the profiles of 60 bright, nearby point sources. It is clear from Figure 1 that the XRB possesses intrinsic (i.e., not due to beam smearing) correlated structure out to angular scales of $\sim 10^\circ$. Full details of the analysis are discussed in Boughn et al. (2002).

3. THE 2–10 keV X-RAY LUMINOSITY FUNCTION

In order to determine the X-ray bias factor b_X from the measured ACF, it is essential to know from which redshifts the X-ray fluctuations originate; the underlying density fluctuations grow quickly, so it is important that they be compared to the X-ray fluctuations at the same redshifts. This requires understanding the contribution to the 2–10 keV X-ray LF as a function of redshift. However, the *HEAO 1* A-2 observations are total intensity measurements of the hard XRB with no information about the fluxes or redshifts of individual sources, so we must infer the LF by other means. Recently, *Chandra* has made possible large, faint hard X-ray surveys with measured redshifts. Cowie et al. (2003) and Steffen et al. (2003) have combined *Chandra* sources with brighter sources from *ASCA* (Akiyama et al. 2000) and *ROSAT* (Lehmann et al. 2001) to determine the redshift evolution of the 2–8 keV LF with few assumptions about the character of the sources. The incompleteness uncertainty in the redshift dependence of the volume X-ray emissivity is estimated to be a factor $\lesssim 2$ at any redshift. The spectroscopically identified sources comprise 75% of the total 2–8 keV X-ray intensity; the dominant uncertainties result from the unknown redshift distribution of the unidentified sources.

Emissivity as a function of redshift, $\lambda_X(z)$, is plotted in Figure 2. The 2–8 keV emissivity in the redshift range $1 < z < 4$ is taken to be that estimated by Cowie et al. (2003) using *ROSAT* data. In the range $0.1 < z < 1.0$, we use the emissivity implied from the luminosity function of Steffen et al. (2003). Finally, for $z = 0$ we use the value of the local emissivity from Miyaji et al. (1994). The models discussed below are based on a polynomial fit that passes through the data points; however, the results are largely independent of the details of the fitted function.

The *HEAO* data are band-limited, and the X-rays detected at high redshifts have larger rest-frame energies than they do locally. Therefore, in order to apply K-corrections to the observed intensities and to transform from 2–8 keV emissivities to the 2–10 keV values appropriate for the *HEAO* map, we must make an assumption about the frequency and redshift dependence of the XRB. If the interstellar medium column density in front of an AGN is large enough ($N_H \gtrsim 10^{21}$ cm^2), the observed spectrum will be hardened by photoelectric absorption. At high redshifts, the rest-frame energies of the detected X-rays are relatively large, and the effect of photoelectric absorption is less.

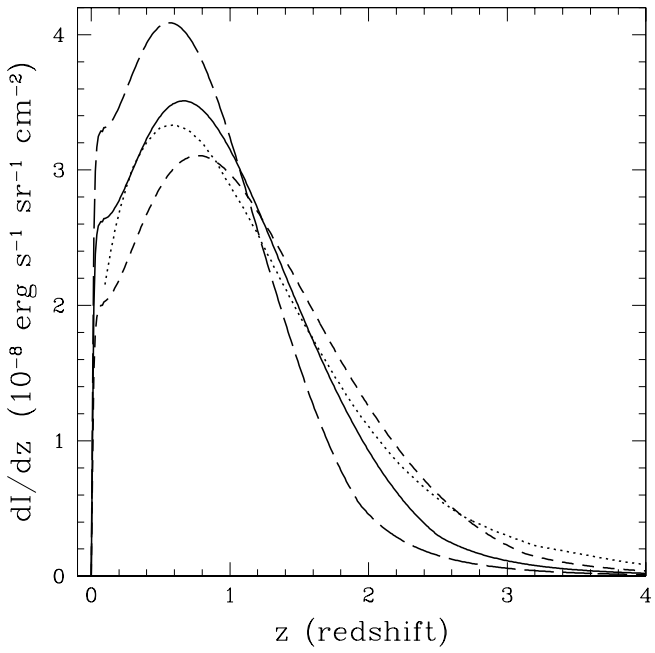

FIG. 3.—Four different models for the contribution to the X-ray luminosity as a function of redshift. The solid line is our best estimate given the volume emissivity. The long- (short-) dashed model results from pushing the emissivity distribution to lower (higher) redshifts. Finally, the dotted line represents the model of Ueda et al. (2003), which is not constrained below $z = 0.1$.

Therefore, for a given column density, sources at high redshift will appear softer than their low-redshift counterparts. As a crude approximation of this effect we assumed a photon spectral index $\Gamma(z) = 1.2 + 0.2z$, where $dN/dE \propto E^{-\Gamma}$ is the number spectrum of the photons of energy E. This roughly describes the redshift dependence of sources with an intrinsic spectral index of $\Gamma = 1.8$ subject to photoelectric absorption by column densities of $N_{\rm H} \sim 10^{22}$–10^{23} cm^{-2}. Furthermore, the flux-weighted average spectral index is $\Gamma = 1.4$, as is observed. The difference between this model and one that assumes a constant spectral index of $\Gamma(z) = 1.4$ is not large, in the sense that the intensity distributions dI/dz of the two models fall well within the range of the extreme models of Figure 3. It is also possible that higher redshift AGNs are more heavily absorbed (e.g., Worsley et al. 2004); however, such effects are not included in some models of the XRB (e.g., Ueda et al. 2003). If the absorption levels were higher at higher redshifts, this would reduce the evolution of the spectral index, i.e., lessen its dependence on redshift. The fact that we observe more energetic rest-frame photons is balanced by the fact that the sources are more absorbed. While neither of the models [constant $\Gamma(z) = 1.4$ or $\Gamma(z) = 1.2 + 0.2z$] is likely to accurately describe the actual spectrum, the fact that the biases of these models are within a few percent of each other indicates that uncertainty in the redshift dependence of the spectral index of the XRB is not an important source of systematic error.

It is straightforward to compute the intensity distribution dI/dz from $\lambda_{\rm X}(z)$ in the context of the ΛCDM cosmological model used by Cowie et al. (2003) ($\Omega_m = \frac{1}{3}$, $\Omega_\Lambda = \frac{2}{3}$, and $H_0 = 65$ km s^{-1} Mpc^{-1}). While this model is somewhat different from that currently favored by the *WMAP* data (Spergel et al. 2003), dI/dz is a directly observable quantity that is independent of the cosmological model. The dI/dz resulting from our canonical emissivity model is given by the middle solid curve in Figure 3, where the normalization is fixed by the LF of Cowie et al. (2003) and Steffen et al. (2003).

This profile implies that the bulk of the XRB arises at much lower redshifts than previously thought (e.g., Comastri et al. 1995), as was first pointed out by Barger et al. (2001). For this particular model, 57% of the 2–10 keV background arises from redshifts less than 1. This is in agreement with the recent observations of Barger et al. (2003) that indicate that 54% of the spectroscopically identified 2–8 keV intensity arises at $z < 1$. This increases to 58% when photometric redshifts are included (Barger et al. 2002, 2003). The total integrated intensity of our canonical model, 5.6×10^{-8} ergs s^{-1} cm^{-2} sr^{-1}, lies between and is consistent with both the *HEAO* estimate of 5.3×10^{-8} ergs s^{-1} cm^{-2} sr^{-1} (Marshall et al. 1980; Gruber et al. 1999) and that estimated from *ASCA* data (Gendreau et al. 1995; Kushino et al. 2002), 6.4×10^{-8} ergs s^{-1} cm^{-2} sr^{-1}. In any case, the current analysis only requires the functional form of dI/dz and not the overall normalization. Finally, the intensity-weighted spectral index of the model, $\bar{\Gamma} = 1.40$, is the same as that observed for the hard XRB (Marshall et al. 1980; Gendreau et al. 1995).

In order to test the sensitivity of the implied X-ray bias to the LF, we consider three alternative models of dI/dz. The top dashed curve in Figure 3 has been weighted to low-z by squeezing (in redshift) the canonical emissivity by a factor of 0.8 while fixing the local emissivity to be the 1 σ upper limit of Miyaji et al. (1994). This model is fairly extreme, as it overestimates the intensity coming from low redshifts. (See Table 1 for a summary of the properties of the various X-ray models.) The lower dashed curve in Figure 3 was weighted to high-z by stretching the canonical emissivity by a factor of 1.3 while fixing the local emissivity to be the 1 σ lower limit of Miyaji et al. (1994). This model significantly underestimates the intensity coming from $z < 1$. Finally, the dotted curve in Figure 3 is from the recent AGN synthesis model of Ueda et al. (2003). Unfortunately, their model of dI/dz did not extend below $z = 0.1$, and our results below depend somewhat on the behavior assumed for low redshifts.

4. MATTER FLUCTUATIONS IN A ΛCDM UNIVERSE AND X-RAY BIAS

Given the X-ray luminosity function, the linear bias factor can be inferred from the cosmological model, but only if the time dependence and scale dependence of the bias are known.

TABLE 1
PROPERTIES OF FOUR MODELS OF X-RAY EMISSIVITY

Parameter	Observed	Best	Low-z	High-z	Ueda et al. (2003)
$f(z < 1)$ (%).....	54/58	57	67	48	52
$b_{\rm X}$	...	1.06	0.86	1.36	1.12

NOTE.—Properties of four models of X-ray emissivity: fraction of the intensity arising from $z < 1$, $f(z < 1)$, and implied bias $b_{\rm X}$. See text for details.

In our analysis we assume both redshift and scale independence of the X-ray bias. Given our nominal intensity distribution, and assuming the standard ΛCDM cosmology, the dominant contribution to the ACF on angular scales of a few degrees comes from structures with redshifts $0.03 < z < 0.5$, which correspond to linear scales of from approximately 10 to 200 Mpc. This is a strong indication that we are observing clustering in the linear regime, and so we can use the straightforward analysis of the growth of linear structures in a ΛCDM universe.

Using the current *WMAP* ΛCDM parameters (Spergel et al. 2003), i.e., $\Omega_m = 0.27$, $\Omega_\Lambda = 0.73$, and $H_0 = 71$ km s^{-1} Mpc^{-1}, it is straightforward to compute a projected matter ACF with the same redshift distribution as for the canonical model (e.g., Boughn et al. 1998). If our assumptions about the bias are correct, the intrinsic X-ray ACF should have the same shape as the normalized matter ACF, with a relative amplitude given by the square of b_X, the X-ray bias factor.

The observed ACF also contains components due to the beam smearing of uncorrelated X-ray sources and photon shot noise, the latter of which is uncorrelated and therefore only contributes to the ACF at $\theta = 0$. Therefore, any fit to the full data set must include these three components. At $\theta = 0^\circ$ the ACF is dominated by beam smearing and photon shot noise, while above $\theta = 12^\circ$ the signal-to-noise ratio is small. The solid curve in Figure 1 is the two-parameter, maximum likelihood fit to the data in the range $2\overset{\circ}{.}5 < \theta < 12^\circ$. The implied X-ray bias is $b_X^2 = 1.12 \pm 0.33$ (1 σ error) or $b_X = 1.06 \pm 0.16$, with a χ^2 of 4.6 for 6 degrees of freedom. Since the distribution of errors in the ACF is to a good approximation Gaussian, the statistical error attached to b_X^2 as well as the χ^2 of the fit have the usual interpretations. The error indicated for b_X represents the 68% confidence interval; however, this error is not Gaussian. The signal-to-noise ratio of the data point at $5\overset{\circ}{.}2$ is 4 σ, and a variety of fits (see below) of b_X^2 to the ACF indicate statistical significances between 3 and 4 σ.

We performed a variety of other fits to the data to check the robustness of our estimate of b_X^2. A three-parameter fit to the data in the full interval ($0^\circ < \theta < 12^\circ$) gives $b_X = 0.96 \pm 0.16$. A one-parameter fit for the large-angle correlations ($5\overset{\circ}{.}2 < \theta < 12^\circ$), where the beam-smearing component is nearly negligible, gives $b_X = 1.20 \pm 0.14$; even a fit to the single datum at $5\overset{\circ}{.}2$ yields a consistent value of $b_X = 1.25 \pm 0.16$, although it is probably mildly contaminated by the beam-smearing component. Following our previous work (Boughn et al. 2002), we also modeled the clustering term as a power law $\propto 1/\theta^\alpha$ with $0.8 < \alpha < 1.6$. These fits varied in amplitude; however, at $\theta = 4\overset{\circ}{.}5$ all of the fits agreed to within a few percent. Normalizing the model clustering ACF to this level implies a bias of $b_X = 1.06 \pm 0.17$, also consistent with our canonical fit. The reduced χ_ν^2 values for these fits are all $\sim$1, and the fits are all consistent with each other.

The process of fitting for large-scale diffuse components and then removing them from the *HEAO* map results in some attenuation of the ACF on angular scales $\gtrsim 10^\circ$. These factors were determined from the same Monte Carlo trials that were used to determine the statistical errors, and the fits were adjusted accordingly. Even if these factors are ignored, the fitted value of b_X changes by only 3%.

To evaluate the level of uncertainty due to a systematic error in the intensity distribution of the XRB, the two "extreme" models of Figure 3 were also fitted to the data in the $2\overset{\circ}{.}5 < \theta < 12^\circ$ interval. The biases resulting from these two fits are $b_X = 0.85 \pm 0.13$ for the low-z model and $b_X = 1.36 \pm 0.21$ for the high-z model. Since these models are somewhat exaggerated, we conclude that they represent lower and upper limits of systematic errors due to uncertainty in dI/dz. A fit to the Ueda et al. (2003) model indicated in Figure 3 results in a similar value of the bias, although the precise results depend on how the model is extended to low redshifts ($0 < z < 0.1$). If this model is extended so that the low-z behavior is not allowed to fall below that implied by Miyaji et al. (1994), $dI/dz = 2.7 \times 10^{-8}$ ergs s^{-1} cm^{-2} sr^{-1}, then the fitted value of b_X becomes 1.12 ± 0.17, which is consistent with that implied by our canonical model. If instead we use a linear extrapolation to low redshifts, the bias can be somewhat ($\sim$15%) higher, but the local emissivity of this model would be nearly 2 σ below that implied by Miyaji et al. (1994).

The ACF on large angular scales is quite sensitive to the contribution of low-z sources (roughly half the ACF at $\theta = 4\overset{\circ}{.}5$ is due to sources with $z \lesssim 0.1$), so any error in estimating the low-redshift cutoff in dI/dz could affect the results dramatically. By masking sources stronger than 3×10^{-11} ergs s^{-1} cm^{-2}, we effectively truncate the intensity distribution at low redshifts. The truncated profiles were determined from the flux cut and the local luminosity function of Steffen et al. (2003). If the value of the flux cut is in error due to, for example, a difference in normalizations of the source catalog used to make the cuts (Piccinotti et al. 1982) and the Steffen et al. luminosity function, then this would affect the cutoff redshift and would be translated to an error in the predicted ACF. In the extreme limit of no flux cut, i.e., no truncation of the dI/dz profile, the implied X-ray bias is $b_X = 0.90$. In the other extreme, i.e., a flux cutoff of 1×10^{-11} ergs s^{-1} cm^{-2}, the implied bias is $b_X = 1.13$. Therefore, it is unlikely that inaccuracy in characterizing the flux cut is the source of significant systematic error.

Potentially more problematic is the redshift distribution of the unresolved component of the XRB. Worsley et al. (2004) found that above 7 keV only $\sim$50% of the XRB is resolved; however, this conclusion must be tempered somewhat by the fact that the brightest sources they considered (in the Lockman Hole) have fluxes of $\sim 10^{-13}$ ergs s^{-1} cm^{-2}. Sources brighter than this contribute to the whole-sky XRB, and Worsley et al. conclude that the true resolved fraction may be 10%–20% higher. Even though only $\sim$20% of the counts in the *HEAO* passband come from photons with energies above 7 keV, an unresolved component can still significantly affect the estimate of the bias. As a pessimistic case, we ignore the bright-source correction and assume a 30% unresolved component below 5 keV. In this case roughly one-third of the 2–10 keV XRB is unresolved. If this unresolved component is distributed in redshift like the resolved component, then there is no change in the implied bias. On the other hand, if the unresolved component is entirely due to sources at high redshift where it does not contribute to the ACF signal, then the implied bias will be 50% higher than our canonical value. If instead the unresolved component is due to sources at low redshift, $z < 1$, then the implied bias will be 20% lower than our canonical value. These fall somewhat outside our two extreme values in Table 1 and so provide a caveat to those estimates of the limits of systematic error. However, if only half of the unresolved component is located at high (low) redshifts and the other half is distributed like the resolved component, then the implied bias is only 20% (11%) higher (lower) than our canonical value, well within the limits of Table 1.

It is difficult to quantify all possible systematic errors; however, considering that the above extremes result in errors

of the same order as the statistical error in the fit, we conclude that the total systematic error is no larger than the statistical error quoted.

5. DISCUSSION

We have determined the X-ray bias of the hard XRB assuming it is time- (i.e., redshift) and scale-independent. These assumptions are probably quite reasonable, since the mean redshift weighting of the X-ray ACF is quite low ($z \sim 0.1$) and the linear scales probed by the ACF are quite large (10–200 Mpc). Even if these assumptions are violated to some extent, b_X can still be interpreted as an "average" X-ray bias. There are several types of sources that contribute to the XRB, including quasars, Seyfert galaxies, LINERS, and clusters of galaxies, and the implied value of the bias must be considered to be an average over all these sources. However, the dominant contribution to the XRB is most likely to be moderately active AGNs (Cowie et al. 2003), so b_X should be representative of the bulk of the sources of the XRB.

With these caveats in mind, we find an X-ray bias of $b_X^2 = 1.12 \pm 0.33$, i.e., $b_X = 1.06 \pm 0.16$ (statistical error only). This error includes photon shot noise, fluctuations in the XRB from beam smearing, and the clustering of the XRB itself. The fits of b_X for two extreme models of dI/dz indicate that the uncertainty due to our ignorance of the X-ray luminosity function is likely less than the statistical error. Other possible sources of systematic error also seem small. We conclude that the hard XRB is a largely unbiased tracer of the matter distribution on large scales. This is consistent with current models of large-scale, late-time galaxy biasing (Benson et al. 2000; Tegmark & Peebles 1998). In addition, the latest studies of the clustering of $\sim L_*$ galaxies on $\sim$100 Mpc scales indicate that these objects are also unbiased tracers of matter. Verde et al. (2002) found that on scales of $\sim$7 to $\sim$40 Mpc, $b = 1.04 \pm 0.11$ for $1.9L_*$ galaxies in the Two-Degree Field survey with a mean redshift of $z = 0.17$. Using a different analysis of the same data, Lahav et al. (2002) found that $b = 1.20 \pm 0.11$ on scales of $\sim$20 to $\sim$150 Mpc. Both of these results are consistent with early findings from the SDSS and 2MASS surveys that imply linear bias factors of order unity (Tegmark et al. 2002; Miller et al. 2003). It should not be surprising that the XRB and galaxy biases are similar, since L_* galaxies are closely associated with the moderately active AGNs that comprise the bulk of the hard XRB (e.g., Barger et al. 2003; Miller et al. 2003).

If these estimates are accurate, then the X-ray bias factor in the linear regime is now much better determined. The hard XRB background appears to be an excellent tracer of the large-scale distribution of matter, making it a useful tool for understanding the evolution of structure in the universe. One example of the importance of determining galaxy biases (and indeed the driving motivation for this work) is to aid in the interpretation of recent detections of correlations of galaxies with the CMB. We (Boughn & Crittenden 2004) have detected a correlation of the 2–10 keV XRB with the *WMAP* map of the CMB (Bennett et al. 2003), and there have been correlations observed with a number of other galaxy surveys (Nolta et al. 2004; Scranton et al. 2003; Fosalba et al. 2003; Afshordi et al. 2004). These correlations have been interpreted as the detection of the integrated Sachs-Wolfe (ISW) effect (Sachs & Wolfe 1967). If confirmed, they would constitute an important test of the ΛCDM cosmological model and provide further evidence of the existence of a substantial amount of "dark energy" in the universe (Crittenden & Turok 1996).

We would like to acknowledge Keith Jahoda, who is responsible for constructing the *HEAO 1* A-2 X-ray map and who provided us with several data handling programs. We also thank Greg Koehrsen for noise analysis programs. R. C. acknowledges financial support from a PPARC AF fellowship.

REFERENCES

Afshordi, N., Loh, Y. S., & Strauss, M. A. 2004, Phys. Rev. D, 69, 083524
Akiyama, M., et al. 2000, ApJ, 532, 700
Bahcall, N. A., & Soneira, R. M. 1983, ApJ, 270, 20
Barcons, X., Carrera, F. J., Ceballos, M. T., & Mateos, S. 2000, in AIP Conf. Proc. 599, X-Ray Astronomy: Stellar Endpoints, AGN, and the Diffuse X-Ray Background, ed. N. E. White, G. Malaguti, & G. G. C. Palumbo (Melville: AIP), 3
Barger, A. J., et al. 2001, AJ, 122, 2177
———. 2002, AJ, 124, 1839
———. 2003, AJ, 126, 632
Bennett, C. L., et al. 2003, ApJS, 148, 1
Benson, A. J., Cole, S., Frenk, C. S., Baugh, C. M., & Lacey, C. G. 2000, MNRAS, 311, 793
Boldt, E. 1987, Phys. Rep., 146, 215
Boughn, S. 1999, ApJ, 526, 14
Boughn, S., & Crittenden, R. 2004, Nature, 427, 45
Boughn, S., Crittenden, R., & Koehrsen, G. 2002, ApJ, 580, 672
Boughn, S., Crittenden, R., & Turok, N. 1998, NewA, 3, 275
Carrera, F., et al. 1998, MNRAS, 299, 229
Comastri, A., Setti, G., Zamorani, G., & Hasinger, G. 1995, A&A, 296, 1
Cowie, L. L., Barger, A. J., Bautz, M. W., Brandt, W. N., & Garmire, G. P. 2003, ApJ, 584, L57
Crittenden, R., & Turok, N. 1996, Phys. Rev. Lett., 76, 575
Ellis, R. S. 1997, ARA&A, 35, 389
Fosalba, P., Gaztanaga, E., & Castander, F. 2003, ApJ, 597, L89
Fry, J. N. 1996, ApJ, 461, L65
Gendreau, K. C., et al. 1995, PASJ, 47, L5
Gruber, D. E., Matteson, J. L., Peterson, L. E., & Jung, G. V. 1999, ApJ, 520, 124
Kushino, A., et al. 2002, PASJ, 54, 327
Lahav, O., et al. 2002, MNRAS, 333, 961
Lehmann, I., et al. 2001, A&A, 371, 833
Marshall, R. E., et al. 1980, ApJ, 235, 4
Miller, C. J., Nichol, R. C., Gomez, P., Hopkins, A., & Bernardi, M. 2003, ApJ, 597, 142
Miyaji, T., Lahav, O., Jahoda, K., & Boldt, E. 1994, ApJ, 434, 424
Nolta, M. R., et al. 2004, ApJ, 608, 10
Piccinotti, G., Mushotzky, R. F., Boldt, E. A., Holt, S. S., Marshall, F. E., Serlemitsos, P. J., & Shafer, R. A. 1982, ApJ, 253, 485
Sachs, R. K., & Wolfe, A. M. 1967, ApJ, 147, 73
Scranton, R., et al. 2003, Phys. Rev. Lett., submitted (astro-ph/0307335)
Spergel, D. N., et al. 2003, ApJS, 148, 175
Steffen, A. T., Barger, A. J., Cowie, L. L., Mushotzky, R. F., & Yang, Y. 2003, ApJ, 596, L23
Tegmark, M., & Peebles, P. J. E. 1998, ApJ, 500, L79
Tegmark, M., et al. 2002, ApJ, 571, 191
Treyer, M. A., Scharf, C. A., Lahav, O., Jahoda, K., Boldt, E., & Piran, T. 1998, ApJ, 509, 531
Ueda, Y., Akiyama, M., Ohta, K., & Miyaji, T. 2003, ApJ, 598, 886
Verde, L., et al. 2002, MNRAS, 335, 432
Worsley, M. A., Fabian, A. C., Barcons, X., Mateos, S., Hasinger, G., & Brunner, H. 2004, MNRAS, in press (astro-ph/0404273)